

Towards a qualitative understanding of the scattering of topological defects

Carl Rosenzweig

Physics Department, Syracuse University, Syracuse, New York 13244

Ajit Mohan Srivastava

Theoretical Physics Institute, University of Minnesota, 116 Church St. SE, Minneapolis, Minnesota 55455

(Received 15 January 1991)

Head-on collisions of strings, monopoles, and Skyrmions result in 90° scattering. We propose a unified description of these objects (for the global case) as members of a definite class of topological defects. All soliton-soliton pairs that are members of this class scatter at 90° in head-on collisions. Our analysis also shows that the scattered solitons are composed of half-portions of the original solitons. We further predict back-to-back scattering for head-on collisions of a soliton-antisoliton pair at sufficiently high energies. We argue that these qualitative aspects of scattering are common because strings, monopoles, and Skyrmions correspond to various winding-number mappings from S^n to S^n . Our analysis concentrates on the smoothness of the field configurations and may be extendible to the scattering of gauged topological defects. For the case of strings our results lead to an understanding of intercommutivity and the accompanying formation of kinks.

I. INTRODUCTION

Topological defects arise in many areas in physics. In condensed-matter physics flux tubes in type-II superconductors, vortices in superfluid helium, and various topological defects in liquid-crystal systems have been experimentally as well as theoretically investigated.¹ In particle physics and cosmology defects such as cosmic strings and monopoles have played very important roles.² The Skyrmion is one of the most important topological objects in particle physics and provides an alternate description of the nucleon.³

Interaction of these defects with each other has also been extensively investigated. Recently an experimental study of strings and other topological defects in a liquid-crystal system was carried out⁴ with results in agreement with earlier theoretical analysis. Such studies are of crucial importance for models of cosmic strings. For example, it was numerically found that when two strings cross, they interchange partners (i.e., they intercommute).^{5,6} This behavior is essential for the viability of any cosmic-string scenario in the early Universe. If strings do not intercommute, they very quickly dominate the energy density of the Universe. Because of the intercommutivity, bigger loops get chopped into smaller loops. An oscillating loop radiates energy and has a lifetime which is shorter for smaller loops. Thus small loops disappear fast enough solving the overdensity problem for strings. Scattering of strings shows many other interesting features as well.⁵⁻⁸ The interaction of Skyrmions in $3+1$ dimensions is clearly of great significance being interpreted as interaction between nucleons.⁹⁻¹² Skyrmion scattering in $2+1$ dimensions has also been investigated in a recent numerical analysis.¹³ As for monopoles, their interaction has enough theoretical interest to have been the subject of investigations for many years.¹⁴⁻¹⁷

There have been many numerical studies of the scatter-

ing and interaction of topological objects. Strikingly enough in head-on collisions a pair of (local) monopoles,¹⁷ a pair of straight strings,⁵⁻⁸ and a pair of Skyrmions in $2+1$ dimensions¹³ all scatter at 90° (90° scattering for a head-on collision of Skyrmion pairs in $3+1$ dimensions has also been conjectured,¹⁸ see also Ref. 19). In some special cases [Bogomolny-Prasad-Sommerfield (BPS) monopoles^{14,15} and critically coupled strings^{7,8}] this behavior can be understood analytically. There is, however, no unified picture of what seems to be very general behavior for an entire class of topological defects.

In the present work we try to fill this gap by developing, for the global case, a common framework for understanding the qualitative behavior of the scattering of these topological defects. The class of objects we consider are defects which correspond to nontrivial mappings of S^n to S^n for appropriate values of n . In $2+1$ dimensions, for $n=1$ and 2 , respectively, we have vortices and textures. In $3+1$ dimensions for $n=1, 2$, and 3 we have strings, monopoles, and textures. Skyrmions in $3+1$ dimensions for the two-flavor case are an example of such textures and we will refer to these textures generically as Skyrmions. (Textures also occur from nontrivial mappings of S^3 to S^2 . However it is not clear whether our considerations in this paper can be extended for those cases.) Even if certain aspects of our arguments may require stronger justification (say, our arguments for the 90° scattering), we feel that we have identified the common topological features which give rise to the striking behavior observed in the scattering of all these different objects. This is one of our major results.

We show that, for a suitable choice of initial configurations, the scattering processes of strings, monopoles, and Skyrmions (in $2+1$ as well as in $3+1$ dimensions) show identical behavior because these simply reduce to the problem of the scattering of parallel straight strings. We find a very surprising result that in a

head-on collision of a soliton and an antisoliton involving annihilation and recreation of a soliton-antisoliton pair, the soliton and the antisoliton bounce back in their original directions. This behavior is rather unexpected though it was observed in one numerical work on strings.⁶ We find that the same must be true for monopoles and Skyrmions as well. It is important to note that this result applies only when, after the annihilation, another pair is recreated. It will be interesting to check this prediction in numerical simulations by working in the appropriate regime of energies.

We also argue that in a head-on collision a soliton-soliton pair scatters at 90° if the initial configurations of solitons are suitably oriented. Our arguments rely on qualitative aspects of our field-configuration *Ansätze* motivated by gradient energy considerations. Even though we do not have strong justifications for these *Ansätze*, it is remarkable that a common set of arguments seems to apply to the case of all three classes of objects and leads to predictions which are in complete agreement with numerical results.

A further interesting aspect of our analysis for the 90° scattering of solitons is that we naturally find that the scattered soliton consists of half-portions of both the original solitons. This behavior has been previously discussed for monopoles and strings.^{6,15,17} Our analysis provides an explanation of this fact and shows that it is generally true and hence must also be true for Skyrmions. It will be interesting to check this prediction as well in numerical works.

We note that the 90° scattering has been observed for certain dipolar vortices on fluid surfaces,²⁰ where also the scattered vortices are composed of the halves of the original vortices. It will be interesting to see if our analysis can be extended to such systems by identifying some suitable dynamical variable (such as the velocity vector field) as the analog of the phase of the Higgs field.

Based on our results for the scattering of string-antistring pairs, we provide arguments for the intercommuting behavior of strings. We analyze the configuration of a string-antistring at the point of crossing and find that it naturally leads to the formation of "kinks" at the crossing point. These kinks have earlier been discussed in the literature and play an important role in cosmology.

At present our analysis is applicable only to defects formed due to the breaking of a global symmetry. In this case we can associate a gradient energy depending upon how fast the field is varying in the internal space. However, since gauged strings and gauged monopoles scatter at 90° ,^{6,7,8,14,15} we feel that it must be possible to extend our analysis for gauged systems as well. This is also suggested by the fact that gauged objects near their core look like global objects, and our analysis is crucially dependent upon the behavior near the core itself. We are presently working on the investigation of the gauged systems.

The organization of the paper is as follows. In Sec. II we discuss the case of scattering of a string-string pair and of a string-antistring pair. We analyze this case in detail and argue in Sec. III that the case of monopoles and Skyrmions can be simply inferred from the analysis of the scattering of strings. We conclude that all these

objects show the same qualitative features in scattering. Section IV presents our conclusions, where we discuss limitations of our analysis and possible extensions of the model.

II. SCATTERING OF STRINGS

A significant amount of numerical work for the scattering of topological defects focuses on the case of strings primarily because of interest in cosmic strings. Since global strings have a long-range force, as the strings approach each other, they antialign near the crossing point. The overlapping portions of the string-antistring pair annihilate (if relative velocity is not too large) leading to intercommutivity [see Figs. 1(a) and 1(b)]. At the point where strings intercommute, a kink forms which does not straighten immediately.⁵ Intercommutivity was also observed for local strings.⁶

Strings naturally arise in phase transitions where the vacuum manifold (the order-parameter space) for the Higgs field (the order-parameter field) is multiply connected. A closed path encircling a string corresponds to the Higgs field tracing a nontrivial loop in the vacuum manifold. The considerations below are quite general, and we expect them to hold for any cylindrically symmetric global string, but for specificity we consider a model in which a U(1) global symmetry is completely broken by a vacuum expectation value of a complex scalar field Φ . A string solution along the z direction is given by²

$$\Phi(r, \theta) = \rho(r) e^{i\theta} \quad (2.1)$$

and an antistring solution is given by

$$\Phi(r, \theta) = \rho(r) e^{-i\theta}. \quad (2.2)$$

r is the distance in the x - y plane and θ is the azimuthal angle. Thus for a string (antistring) the phase ϕ of the Higgs field at angle θ is $\phi = \theta$ ($-\theta$). The magnitude of Φ is $\rho(r)$ with $\rho(0) = 0$ and $\rho(\infty) = \eta$, the vacuum expectation value of Φ .

A. String and antistring parallel to z direction: back-to-back scattering

Our analysis assumes that the qualitative aspects of scattering are determined by the consideration of the gradient energy associated with the phase variation of the

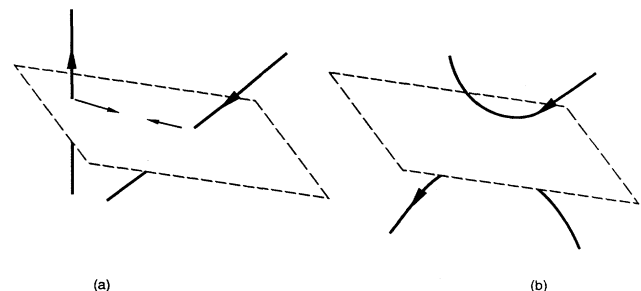


FIG. 1. Intercommutivity of strings.

Higgs field. Because of the z symmetry we can ignore the z direction and simply consider the field configuration in the x - y plane. The following results also apply to the scattering of vortices in two spatial dimensions.

Consider the initial configurations as shown in Figs. 2(a) and 2(b). If the string and antistring are sufficiently far, the contours of constant Higgs field phase ϕ will be straight lines radially emanating from the respective centers of string and antistring. Black dots in the center of the string (antistring) represent $\Phi=0$ region. Though the constant phase lines go to infinity, the magnitude of the Higgs field $\rho(r)$ will differ considerably from the vacuum value η only in a small region shown in Figs. 2(a) and 2(b) by circles encircling the centers of the string and the antistring. (However, we point out that this region, where the gradient energy due to the radial derivative of the Higgs field is concentrated, does not play any role in our analysis.)

Figure 3(a) shows the field configuration as the string and antistring approach each other. If one of them (say the antistring) was initially rotated in the x - y plane compared to Figs. 2(a) and 2(b), due to phase-gradient energy we expect it to develop into a configuration such as in Fig. 3(a). Figure 3(b) shows an intermediate stage of annihilation where the string and antistring partially overlap. We emphasize that what we are presenting are the *Ansätze* for the annihilation process motivated by an appropriate gradient energy term. (As far as the continuity properties of the field configuration are concerned, our *Ansätze* are similar to those used in Ref. 21.) Figure 3(c) shows total annihilation when the centers of the string and antistring completely overlap.

Of course, as the string- and antistring approach each other, we expect the contours of constant phase ϕ to deform in order to minimize gradient energy. This is depicted in Fig. 4(a). Since contours of constant ϕ will try to concentrate in the region between the pair, we expect that when the centers of the string and antistring overlap, the field configuration looks like Fig. 4(b) as opposed to Fig. 3(c). Here θ is some angle between 0 and $\pi/2$ [for Fig. 3(c), θ is equal to $\pi/2$].

In Fig. 4(b) the centers of the string and antistring (which are characterized by $\Phi=0$) overlap, the string and antistring have annihilated and all the energy may go in radiation. [Note that in Fig. 4(b) there is no loop which has a nontrivial winding number.] We are, however, interested in a different situation in which another string-

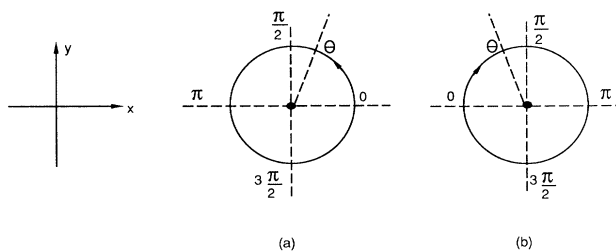


FIG. 2. (a) The configuration of a string in the x - y plane; (b) the configuration for an antistring.

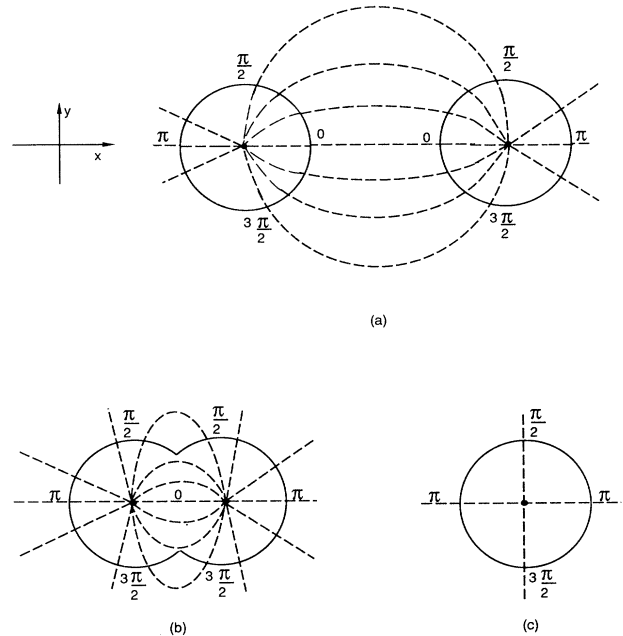


FIG. 3. Field configuration at various stages of the annihilation of a string-antistring pair. (c) The stage of total annihilation when the two centers of the string and antistring have overlapped.

antistring pair is recreated after the annihilation. Thus the issue we have to address is, given the field configuration in Fig. 4(b) and given that a string-antistring pair will be recreated from this configuration, whether we can get information about the direction in which the string and the antistring are most likely to separate.

Suppose that the string and antistring separate away from the dotted line in Fig. 5(a). This line intersects the circle (in which Φ differs significantly from η) at two points where the Higgs field has phase ϕ equal to $\pi-\alpha$ and $\phi=\pi+\alpha$. Here angle α is between 0 and θ . A pair is created as soon as the string and antistring separate just enough that they have distinct centers. Figure 5(b) shows this pair separating along the line perpendicular to the dotted line of Fig. 5(a). Each pair has a portion, shown by a solid arc, which represents the field configuration at the time of annihilation. We assume that this configuration is not significantly changed by very small separa-

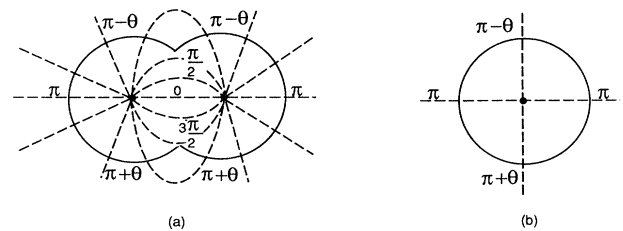


FIG. 4. The same as in Figs. 3(b) and 3(c) but now the distortions of contours due to gradient energy is taken into account. Here θ is between 0 and $\pi/2$.

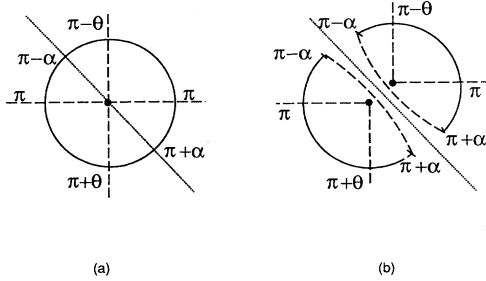


FIG. 5. Creation of a new string-antistring pair from the configuration of Fig. 4(b). The string- and antistring separate away from the dotted line. (b) The situation when the two pairs have well-defined separate centers (in the sense that ϕ has non-trivial winding numbers around small loops encircling these centers). α is between 0 and θ .

ration of the centers. The distribution of the phase ϕ on dashed arcs is not fixed by the knowledge of the configuration of Fig. 5(a) and will determine which one is a string and which one an antistring.

Consider first the case when the string is separating towards the lower left half of the x - y plane and the antistring is separating towards the upper-right-half plane. Since the initial string-antistring pair was moving along the x axis [see Fig. 3(a)], this represents a string and antistring bouncing back in their own half planes. Figure 6(a) shows the values of the phase ϕ at various points along the dashed portion of the separating string which are required in order to have winding number one. The important thing to note is the sequence of the occurrence of these values for ϕ . Let us trace the loop around the string starting at the point p in Fig. 6(a). As we trace this loop counterclockwise in the x - y plane, the phase ϕ traces a closed curve in the vacuum manifold S^1 as shown in Fig. 6(b). As we go around the circle in the x - y plane the Higgs field phase ϕ completes unit winding number along S^1 , but ϕ does not increase monotonically. A portion of the vacuum manifold (between $\phi = \pi + \alpha$ and $\phi = \pi + \theta$) is retraced when $\alpha \neq \theta$. Thus the configuration of the string is a highly excited one with more gradient energy than, for example, the string in Fig. 4(a). Clearly the same is

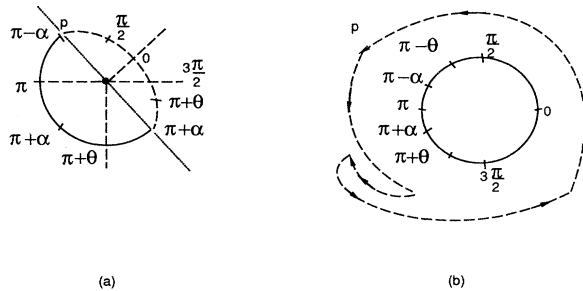


FIG. 6. (a) The distribution of ϕ on the dashed-arc portion needed in order to represent a string. (b) The path traced in the vacuum manifold as a closed loop is traced counterclockwise (a) starting at p .

true for the antistring as well. (Since the separation of the centers of the string and antistring is very small at this stage, we assume that the phases at various points on the dashed portion of the antistring will be the same as the ones at the corresponding points on the dashed portion of the string.)

Now consider an antistring separating in the lower-left-half plane and string in the upper-right-half plane. Figure 7(a) shows the values of ϕ required in the dashed portion of the antistring and Fig. 7(b) shows how ϕ varies along S^1 when a closed loop is traced counterclockwise starting at point p in Fig. 7(a). We again see that a portion of the vacuum manifold (between $\phi = \pi - \alpha$ and $\phi = \pi + \theta$) is retraced. The same is true for the string that is separating in the upper-right-half plane.

At this step we may draw some conclusions from these figures. We see that for Fig. 7(a), any value of α leads to a highly excited string-antistring pair, whereas for Fig. 6(a), the string-antistring pair has a higher gradient energy [as compared to the case in Fig. 4(a)] as long as $\alpha \neq \theta$. In order to have the lowest gradient energy we may expect that the configuration that requires least variations of the field (in the sense that no portion of the vacuum manifold is retraced) will be preferred. Intuitive arguments thus single out the value of $\alpha = \theta$ for Fig. 6(a) which corresponds to back-to-back scattering of the string-antistring pair. In simple terms we are saying that in the left-half portion in Fig. 4(b) the phase ϕ already winds partially in the anticlockwise direction (corresponding to a portion of the string), and it will cost extra gradient energy to reverse this direction if this configuration is to separate out as an antistring with ϕ having a net winding $= -1$.

A rough estimate of the gradient energy densities [coming from a term such as $(\nabla\Phi)^2$ in the Lagrangian] can be made as follows. We consider only some sort of average gradient energy densities and assume that it gives a fair representation of the net gradient energy of the field configuration. An actual calculation of the net energies requires the knowledge of the details of field configuration even far from the cores of the string and cannot be done in the present qualitative framework. Since we are only interested in the comparison of energies for various possible configurations, we believe our approxi-

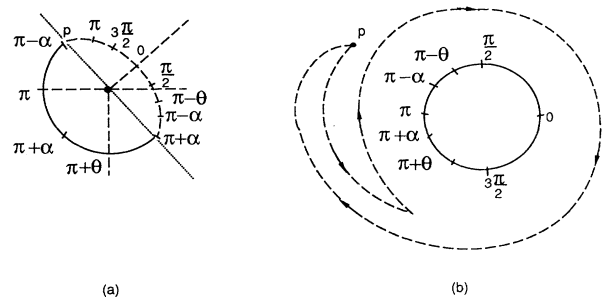


FIG. 7. Same as in Fig. 6 but now the values of ϕ on the dashed arc are chosen so that the configuration (a) represents an antistring.

mations are fairly justified. First consider the case in Fig. 6(a). We have

$$E_1 \simeq \left[\frac{2\alpha + 2(\theta - \alpha)}{l/2} \right]^2 + \left[\frac{2\pi - 2\alpha}{l/2} \right]^2 \\ = \frac{16}{l^2} [\theta^2 + (\pi - \alpha)^2], \quad (2.3)$$

where the first term is the gradient energy density for the solid-arc portion in Fig. 6(a), and the second term is for the dashed-arc portion. l denotes an appropriate arc length for both halves (which are separated by the dotted line). (For this one may replace the solid arc by an arc which has roughly the same shape as the dashed arc.) Here we have assumed uniform variation of the phase ϕ for the solid-arc portion as well as for the dashed-arc portion. As we are interested in rough comparative estimates, we expect this approximation not to qualitatively affect our results. We again emphasize that we are simply estimating some sort of average gradient energy density. For example, the same value as in Eq. (2.3) will be obtained by considering the antistring configuration. If we were to calculate net gradient energy, we will have to estimate the sizes of various regions near as well as far from the centers.

Similarly, the gradient energy density E_2 for the case in Fig. 7(a) is

$$E_2 \simeq \left[\frac{2\alpha + 2(\theta - \alpha)}{l/2} \right]^2 + \left[\frac{2\pi + 2\alpha}{l/2} \right]^2 \\ = \frac{16}{l^2} [\theta^2 + (\pi + \alpha)^2]. \quad (2.4)$$

Since $0 \leq \alpha \leq \theta$, we see from Eqs. (2.3) and (2.4) that the lowest gradient energy is obtained for the case of Eq. (2.3) with $\alpha = \theta$. This represents back-to-back scattering, which is clear from Fig. 5(b). In fact it is clear from Eqs. (2.3) and (2.4) that the gradient energy keeps increasing as the angle of scattering is decreased from π (exactly back-to-back scattering) to zero (exactly forward scattering).

This is a remarkable result. If the dynamics of the annihilation (and recreation) of a string-antistring pair is dominated by phase-gradient energy considerations, then the string and the antistring will bounce back after colliding head on. This is especially surprising as the string and antistring attract each other. We believe this provides an explanation of the numerical result in Ref. 6 where a brief mention of this behavior was made.

We will now turn to the case when the string and antistring are not exactly parallel. We will argue that above considerations may provide a clue to the intercommuting behavior of strings.

B. Intercommutivity of strings

Intercommutivity of strings means that a pair of strings, while crossing, exchanges partners [Figs. 1(a) and 1(b)]. It is clear from these figures that for a pair of strings at any angle (except when they are exactly parallel) we can always find a plane through the point of inter-

section such that along any loop in this plane encircling the intersection point the winding number of the Higgs-field phase ϕ is zero. This plane is shown by dashed lines in Figs. 1(a) and 1(b) (see also Shellard in Ref. 6). The region near the intersection point, therefore, is topologically trivial, and the strings may pinch off at that point separating away from the plane. Strings have intercommuted. Thus the consideration of string-antistring crossing is completely general and amounts to an appropriate choice of coordinate frame. During crossing, a segment of string and antistring overlaps completely. For the case in Figs. 1(a) and 1(b) this leads to strong twisting as the string and antistring approach each other. For this reason, we consider crossing in a plane where it is easier to keep track of the phase ϕ around the string and antistring. The considerations can be extended to the case of Figs. 1(a) and 1(b) without altering any conclusions.

Consider the crossing shown in Figs. 8(a)–8(c). We show the thick core of the string as well as the variations of the phase ϕ on loops enclosing these strings. Figure 8(b) represents the situation where at the midpoint of the crossing, the string and antistring are completely overlapped. Figure 8(c) shows the stage when the middle portions have crossed. Figures 8(a)–8(c) thus represent the situation where the strings have not intercommuted.

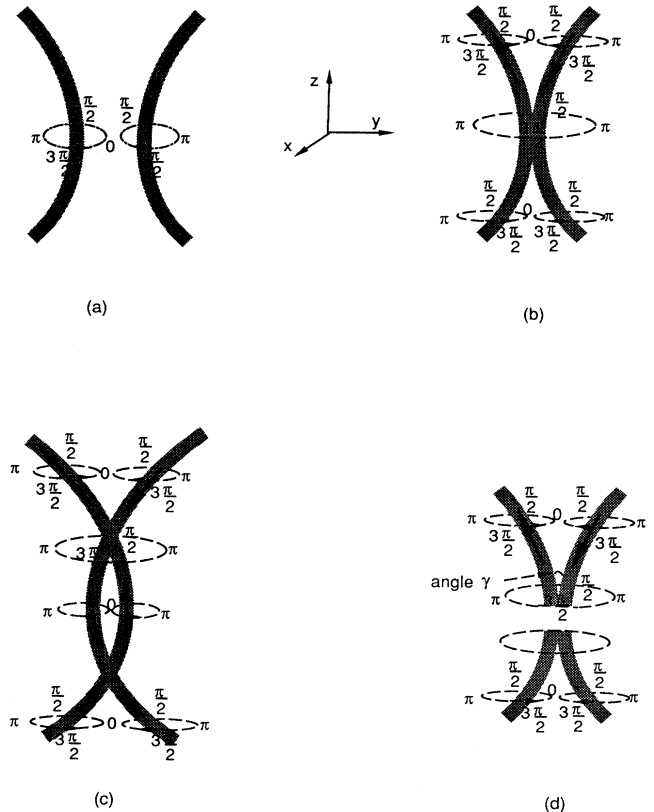


FIG. 8. Crossing of strings. (b) A certain segment of the string and antistring have overlapped. (c) The case when strings cross each other, and (d) the case when strings intercommute by pinching of the middle portion (b).

Strings will intercommute if instead of evolving into the configuration shown in Fig. 8(c), the configuration of Fig. 8(b) evolves into the one shown in Fig. 8(d). We see in Fig. 8(d) that this configuration is obtained from Fig. 8(b) by the pinching of the loop in the middle of the crossing (note that it is a topologically trivial portion of the configuration).

If we consider the cross sections of the string and antistring in the x - y plane at $z=0$, we see that Figs. 8(a)–8(c) represent the sequence of events analogous to the one shown in Figs. 3(a)–3(c) with Fig. 8(b) representing the case of complete annihilation [as shown in Fig. 3(c)]. Figure 8(c) then represents the case when another string-antistring pair is created in the forward direction, while Fig. 8(d) shows the case when the portion where the string and antistring were completely overlapped in Fig. 8(b) radiates its energy in Goldstone bosons and disappears, thereby pinching off the string. In Fig. 8(c), we have shown only 0 and π values of ϕ at the midpoint of the crossing, because the lines representing other values will be twisted in a more complicated fashion [see Fig. 7(a)]. Also for simplicity we have chosen to work with the case shown in Figs. 3(a)–3(c) as compared to the more appropriate case of Figs. 4(a) and 4(b). This does not affect our qualitative arguments following.

As we argued in Sec. II A, forward scattering of a string-antistring pair requires higher gradient energies and hence is not preferred. If the strings do not intercommute, then we are led to Fig. 8(c). Let us just follow the phase variations around (say) a string as we go along it. We see that there is a twist in the $\phi=0$ line on the string by π as we approach (along the z axis) the center of the crossing point (from below), and as we go further up the string gets untwisted. Clearly this twist requires an extra amount of gradient energy. The same twist is also present in the antistring. A rough estimate of the extra gradient energy density due to this twist can be made (say, for an antistring) as follows.

Note that crossing does not require exact forward scattering and one only needs, after overlapping, for the string and antistring to go in the other half plane than they were in before scattering. Hence consider the antistring configuration of Fig. 7(a). Since the line of Higgs phase $\phi=0$ for the initial antistring was along the negative x axis [see Fig. 3(a)], the angle δ by which this $\phi=0$ line has twisted in Fig. 7(a) is

$$\delta = \frac{\pi\alpha}{2\theta} + \frac{\pi}{2}. \quad (2.5)$$

Here we have assumed that the variations of ϕ in the solid-arc region, as well as in the dashed-arc region, are uniform.

The lines of ϕ for other values will twist by a different (and possibly smaller) amount. The important thing is that all such lines will be twisted for the crossing shown in Fig. 8(c). We use the above value of δ to get a rough idea of the average twist in the string. This leads to a contribution $\simeq k\delta^2$ to the gradient energy density from a term such as $(\nabla\Phi)^2$. (Here k is some constant.) Also, since this corresponds to forward scattering, there is an extra contribution to the gradient energy density from

Eq. (2.4). Thus, the net contribution to the gradient energy density is

$$E_{\text{gradient}} = \frac{16}{l^2} [\theta^2 + (\pi + \alpha)^2] + \frac{k\pi^2}{4} \left[\frac{\theta + \alpha}{\theta} \right]^2. \quad (2.6)$$

It is seen immediately from both the terms in the above expression that the gradient energy increases with increasing α . Essentially this means that when the strings cross, their gradient energies become very large, making the crossing of strings less favored as compared to intercommutivity. Of course, strings could bounce back as then there is no twist energy and also the gradient energy contributions will be minimal [see Eq. (2.3)]. However, for two long strings crossing in a small region, the momentum of strings will not allow strings to bounce back. As we have argued above, the distribution of phase ϕ near the crossing point will favor that the strings intercommute (i.e., the overlapping region of the string and antistring will pinch off). It should be possible to compare the increase in the gradient energy [Eq. (2.6)] with the kinetic energies of the relevant portions of the string (i.e., the portion near the crossing point) and get some idea of the magnitude of critical velocity of the strings beyond which the contribution of Eq. (2.6) becomes irrelevant and strings can freely cross. However we will not get into such an investigation in this paper.

C. Kink formation

We have seen above that intercommutivity of strings results when the configuration of Fig. 8(b) evolves into the configuration of Fig. 8(d), which is obtained by letting the middle portion of Fig. 8(b) disappear. It is known from the numerical studies of global strings that due to long-range forces, the strings try to antialign near the crossing point.⁵ We expect this to be generally true in order to have a smooth field configuration near the crossing point. (Of course the length of the portion where the strings are exactly antialigned will be smaller for the case of gauged strings.) Thus the angle γ in Fig. 8(d) between the string and antistring will be expected to be very small. (In fact we expect γ to approach to zero as the midpoint of the overlap is reached.) It is very suggestive to identify this configuration as the kink. The difference between this configuration and any other normal “bend” in the string as shown in Fig. 9(b) can be seen by noticing the following. At the point of maximum curvature for the bend in Fig. 9(b), the tension of the string acts tangentially and tries to straighten the bend. Such a bend will thus very quickly disappear due to string tension. Contrary to this the string tension in the configuration of Fig. 8(d) has no tendency to straighten the kink as is clear from Fig. 9(a). Since the strong attraction of the string and antistring keeps the angle γ as small as possible in Fig. 9(a), the tension becomes less and less effective for straightening the kink.

We thus expect that the configuration of Fig. 9(a) has much greater stability as compared to normal bends of the string and looks and behaves quite similar to the kinks. Actually if the bend of Fig. 9(b) is made sharper and sharper, it will eventually result in a kink when the

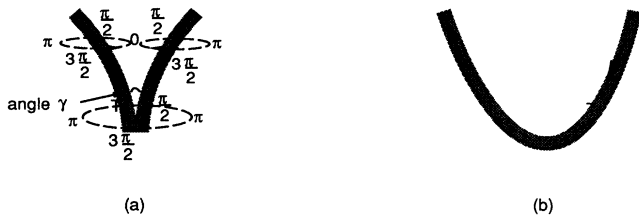


FIG. 9. (a) The configuration of the string near the point where the strings intercommute. (b) A normal bend in a string. T here denotes the string tension.

inner sides of the string and antistring fuse together. It will be extremely unlikely to form such fused configuration by bending an initially straight string due to large tension. However, we find that intercommutivity naturally leads to such fused configurations (kinks).

D. String and string parallel to z direction: 90° scattering

We consider strings parallel to the z axis and again, because of z symmetry, concentrate on the $z=0$ cross section of the strings. Figure 10 shows a well-separated pair of strings with a suitable choice of orientation. Figure 11(a) shows an intermediate stage of scattering, and Fig. 11(b) shows the stage when the overlap of the two strings is maximum. We emphasize that our considerations below depend crucially upon the existence of the stage shown in Fig. 11(b), where the centers of two strings have completely (or almost completely) overlapped. Since parallel strings repel each other, such a stage will not occur if initial kinetic energies of strings are small. Thus this analysis is applicable only for certain energy regimes.

The aspect of the configuration of Fig. 11(b) which is most crucial to our analysis is the following. The dashed lines which represent contours of constant Higgs-field phase ϕ are most dense along the line PQ which is perpendicular to the line RS representing the direction of approach of the two strings. Density of these contours slowly decreases as we rotate the line PQ to the line RS and is lowest near the line RS . This behavior is very natural to expect and follows from the fact that the forces responsible for the distortion of the contours decrease with increasing distance. Thus each string is not able to significantly affect the distant portions of the other string. Also the phase distribution shows that the phase ϕ is constant on the dashed lines even when we cross the center of the strings. We have considered a symmetrical configuration here in which the line of constant phase ϕ are most dense along the line PQ perpendicular to the

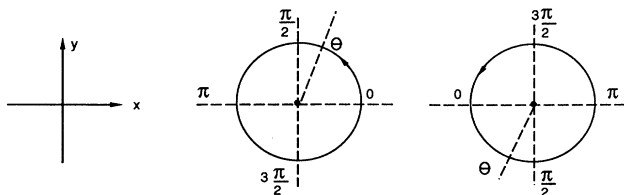


FIG. 10. A far-separated pair of strings.

original direction of approach. It seems to us that if while colliding the strings were not symmetrical, then one will not obtain 90° scattering, and the strings will then scatter in the direction along which the lines of constant phase are most dense. We assume that in an exactly head-on collision, the strings orient themselves so that a configuration like Fig. 11(b) is achieved.

Because of the symmetry of the problem, the strings can only separate either along the x axis (i.e., along the line RS) or along the y axis (i.e., along the line PQ). If the strings were to separate along, say, a line making the angle $-\theta$ from the y axis, then they should also be able to separate along a line making the angle $-\theta$ from the y axis, since the configuration has reflection symmetry about the y axis (as well as about the x axis). Since we are studying the evolution of fields governed by classical equations of motion, such ambiguity cannot occur. This ambiguity is absent only along the x axis or along the y axis.

Now suppose we maintain this reflection symmetry about the y axis (and x axis) but smoothly change the concentration of the contours of constant phase ϕ by a very small amount. As long as we do not alter any qualitative aspects of the configuration of Fig. 11(b), we expect that the two strings will still separate along the same axis as before. The qualitative aspects of this configuration

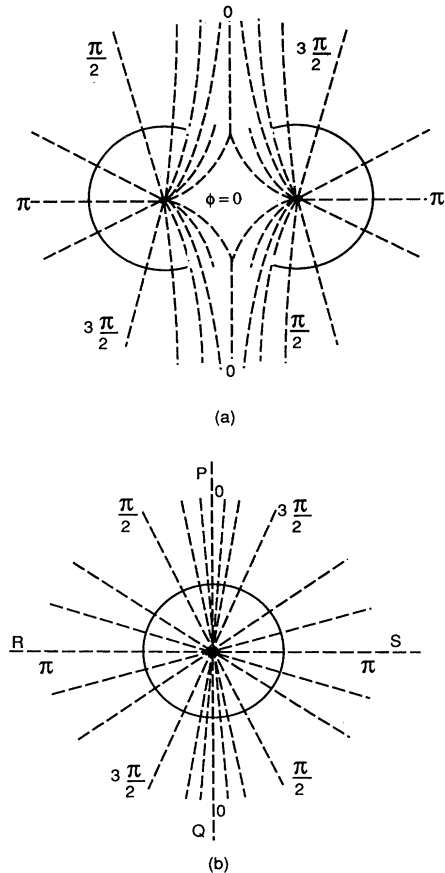


FIG. 11. (a) An intermediate stage in the scattering of two strings, and (b) the stage when the two strings completely overlap.

are (1) reflection symmetry about the y and x axes and (2) concentration of the contours of constant ϕ along the y axis. As we mentioned, as long as the reflection symmetries about the y and x axes are maintained, the only possible directions for separation are the x and y axes. [One can construct configurations in which the possibility is enlarged to a larger number of directions, but such configurations will not be relevant to the situation shown in Fig. 11(b).] Since the x and y axes have a discrete value of angle ($\pi/2$) between them, we do not expect that the separation direction suddenly jumps from one axis to the other by a very small deformation of the field which still preserves the qualitative aspects (1) and (2).

Of course by deforming the field further and further so that the variation of ϕ is more and more uniform (and not concentrated near the y axis), we will reach a situation when the ϕ variation is completely isotropic. At this point the qualitative aspect (2) changes discontinuously in the sense that continuing the same type of deformation, we will reach a situation when the ϕ variation is more concentrated near the x axis. Since one of the qualitative aspects of the figure has now changed discontinuously, we have no reason to believe that the direction of separation still should be the same as before. Therefore a jump in the direction may be allowed now.

Analogy between these arguments and the standard topological arguments should be clear by now. Our arguments are similar to those used for showing the winding number to be a topological invariant. If we know that a certain integral (of fields) has only integer values, then continuous small deformations of fields cannot change this value. Small changes should not lead to discrete jumps if continuity is maintained. Our direction of separation of two strings, which for Fig. 11(b) has only two (discrete) possibilities (x and y axes), is the analog of the winding number. The conditions of continuity are less clear in our case. Our arguments amount to saying that any change of fields which maintains the qualitative aspects of the configuration should be considered as a continuous change.

Following the above line of arguments, let us consider the following deformation of the configuration of Fig. 11(b). Deform the field so that the dashed lines of constant phase ϕ are more and more concentrated along the y axis. This does not change any of the qualitative aspects (1) and (2). Deforming the fields more and more we arrive at the configuration shown in Fig. 12(a), where the phase ϕ is completely constant ($=\pi$) in the region away from the y axis and ϕ changes by 2π across the positive y axis as well as across the negative y axis (full variation around the origin is 4π). According to our above arguments the direction of separation of strings in Fig. 12(a) will be the same as the direction of separation for Fig. 11(b).

Figure 12(a) represents the case when the full gradient energy of the two strings is concentrated along the y axis (in the y - z plane if the z direction is taken into account). Clearly in this case the motion of the strings will be to shorten the length of the "stringlike region" along the y axis. For this purpose one may imagine antistrings at $y = \pm\infty$ also parallel to the z axis. Thus in the full three-

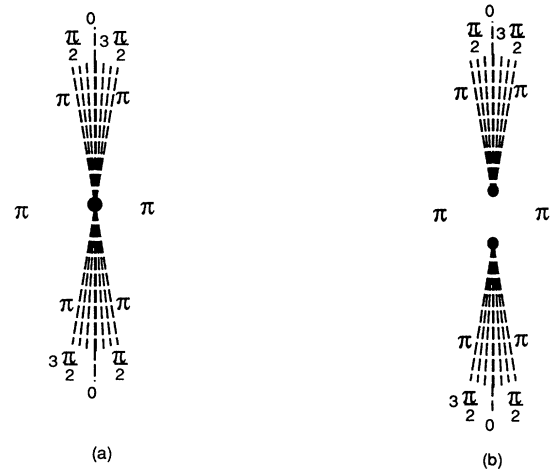


FIG. 12. (a) A deformation of the configuration of Fig. 11(b). Here the phase ϕ is constant ($=\pi$) away from the y axis and changes by 2π across positive y axis as well as across the negative y axis. (b) The expected evolution of the configuration (a). Here the two strings are separating along the y axis.

dimensional problem Fig. 12(a) will represent two strings at the origin connected by a sort of domain wall (in the y - z plane) to two antistrings at $y = \pm\infty$. [For the two-dimensional problem Fig. 12(a) represents two monopoles at the origin connected by strings to two antimonopoles at $y = \pm\infty$.] Clearly the two domain walls will try to decrease their areas by moving the two strings along the $+y$ axis and $-y$ axis. Thus the configuration of Fig. 12(a) will evolve into the configuration shown in Fig. 12(b) which represents the two strings scattering at 90° to the original direction of approach. As we argued above, the configuration of Fig. 12(a) is the same as the configuration of Fig. 11(b) as far as the qualitative aspects (1) and (2) are concerned; hence, we conclude that for Fig. 11(b) as well, the two strings will separate along the y axis, i.e., at 90° to the original direction of approach. Figure 13 shows this pair of strings separating along the y axis.

We thus conclude that when two strings scatter in a

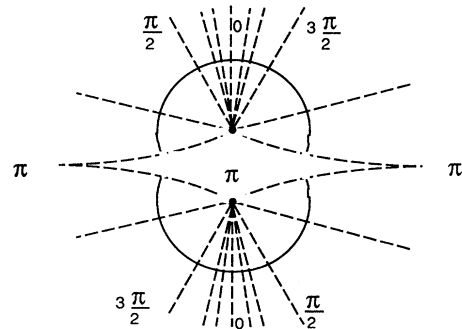


FIG. 13. Configuration of Fig. 11(b) evolving into two strings separating along the y axis (which is at 90° to the original direction of approach).

completely symmetrical manner, they are most likely to separate out at 90° to the original direction. Another very interesting aspect which is very natural from Figs. 11(b) and 13 is that the right half of the string, which is going in the upper direction, is formed from the top half of the original string coming from the right and the left half of that string (which is going in the upper direction) comes from the top portion of the left initial string. Similarly the string which is going to the lower direction consists of lower halves of the initial strings. This behavior is consistent with various numerical results.^{5,6}

III. SCATTERING OF MONOPOLES AND SKYRMIONS

We now discuss the cases of monopole and Skyrmion scatterings. We will show that for suitable choices of initial configurations, these scatterings can be understood in terms of the results obtained for strings.

A. Monopole scattering

Monopoles are formed when there are nontrivial mappings from a two-sphere S^2 into the vacuum manifold of the Higgs field. We will consider the case when the vacuum manifold is S^2 [as is the case when $SU(2)$ symmetry is spontaneously broken to $U(1)$ symmetry]. Figure 14(a) shows a monopole configuration. At the origin the Higgs field $\Phi=0$, and Φ goes to its vacuum value η far away from the origin. The internal directions of Φ on a two-sphere S^2 enclosing the origin are shown in Fig. 14(a). The internal degree of freedom for Φ is characterized by two angles Θ (between 0 and π) and Ψ (between 0 and 2π) since the vacuum manifold for Φ is S^2 .

In Fig. 14(a) we have divided S^2 into a family of circles, each parallel to the equator. The angle Ψ winds once around each of these circles (thus all of these circles represent a winding-number-one mapping of S^1 to S^1). These circles are further characterized by the angle Θ . Θ is 0 at the north pole and $\Theta=\pi$ at the south pole of S^2 ($\Theta=\pi/2$ for the equatorial circle). We have here used a standard way of constructing the winding-number- n map of S^P to S^P , wherein one starts with a winding number n map of S^{P-1} to S^{P-1} . By considering S^P as the suspension of S^{P-1} , this map is then extended to a map from S^P to S^P which can be shown to be a winding number n map (see Refs. 21–23).

Figure 14(b) shows an antimonopole configuration. The only difference between Fig. 14(a) and 14(b) is that now all the circles (which are parallel to the equator) represent a winding-number-minus-1 map of S^1 to S^1 . Thus Ψ varies in the opposite direction along these circles as compared to the case of Fig. 14(a), whereas variation of Θ from the south pole to the north pole remains the same as before. In these figures we have shown the variation of Ψ by dotted lines for a circle in the lower half of S^2 . Variation of Ψ for other circles (for different values of Θ) will be the same.

Now let us study the scattering of a monopole-antimonopole pair. Figure 14(c) represents an intermediate stage of annihilation where the two S^2 's have partially overlapped. We have again oriented the monopole-

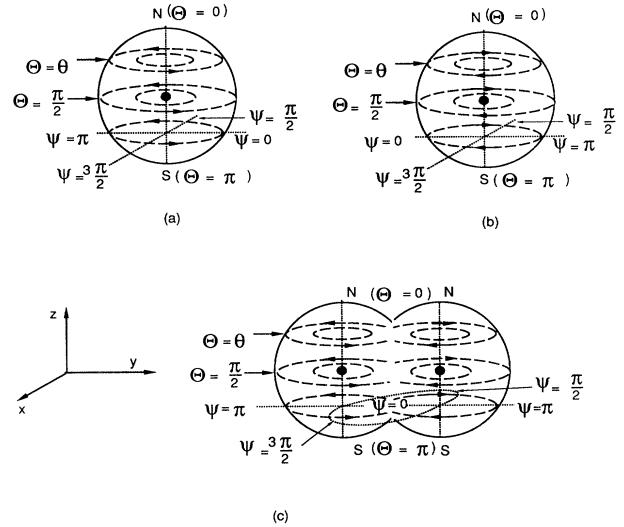


FIG. 14. (a) A monopole and (b) an antimonopole configuration which are our initial configurations for a far-separated pair. (c) An intermediate stage of the annihilation of the monopole-antimonopole pair.

antimonopole pair in a very symmetric fashion, as this is what we expect the gradient energy to lead to. As in the case of strings, the S^2 's shown here represent regions around the centers of the monopole and the antimonopole, where the Higgs field Φ differs significantly from its vacuum expectation value η . Again our considerations do not depend upon this S^2 . Rather they depend on the variation of Ψ and Θ , which is the same for all S^2 's concentric with the respective centers of the monopole and the antimonopole.

By comparing Figs. 14(c) and 3(b) for the case of the scattering of the string-antistring pair, we see that as far as matching of Ψ is concerned, the two situations are identical. As for Θ , as long as the motion of the monopole-antimonopole pair remains confined in the x - y plane for scattering with zero impact parameter, Θ matches smoothly for various circles on the S^2 's of the monopole and antimonopole. Thus Θ becomes an irrelevant parameter for this kind of scattering. It is then straightforward to repeat the considerations of Sec. II A for this case, and we are led to exactly the same conclusions as the ones in Sec. II A. We, therefore, conclude that for the configurations of monopole-antimonopole as shown in Fig. 14(b), the monopole-antimonopole pair will bounce back if another monopole-antimonopole pair is recreated after the annihilation. This behavior has not yet been observed in numerical studies. However, as should be clear from the above analysis that this result is expected under rather restricted conditions which are (1) exact symmetry of the configurations so that the motion remains in the x - y plane (i.e., a plane which is parallel to the circles that have nontrivial winding number), and (2) energy should be large so that after the annihilation, another pair could be easily created. It will be very interesting to check this prediction by working in the appropriate energy regime.

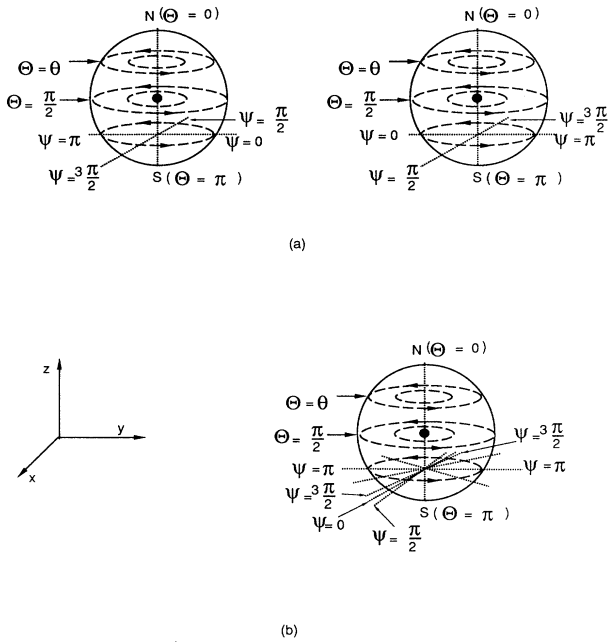


FIG. 15. (a) A pair of far-separated monopoles. (b) The stage when the two monopoles are completely overlapped.

Let us now consider the case of monopole-monopole scattering. Figure 15(a) shows two far-separated monopoles, and Fig. 15(b) shows the stage when the two monopoles are completely overlapped. Again the analogy between this case and the string-string case as shown in Figs. 11(a) and 11(b) is quite clear. Note that the variation of Ψ (shown by dotted lines for a circle in the lower half of S^2) is maximum along the x axis and gradually decreases as we rotate to the y axis. The situation is identical to the one shown in Fig. 11(b) [with x - y axes interchanged as the direction of approach in Fig. 15(a) along the y axis]. Thus the variation of Ψ is maximum across the x - z plane here [same as for Fig. 11(b) where the phase variation was maximum across the y - z plane].

Following the analysis of Sec. IID we thus conclude that if the collision is energetic enough such that the centers of monopoles completely overlap, then the monopoles will scatter at 90° with respect to the original direction of motion. Again due to the symmetry of the problem, the motion of the monopoles is confined in the x - y plane (which is determined by the planes of the circles with nontrivial winding number for Ψ). We further note that according to the analysis of Sec. IID, the configuration of the scattered monopole which is going in the negative x direction (positive x direction) is composed of those half-portions of the initial monopoles which were in $x < 0$ ($x > 0$) regions of the space. These findings are completely consistent with earlier results.¹⁵

The essence of the arguments we have used above is that the scattering of monopoles can be reduced to the case of the scattering of strings if the monopoles are appropriately oriented. The reason that we are able to do so is clear from the above construction of the monopole configuration, which is simply obtained by considering a

family of circles, all of which are just like the string configuration. Once the label (Θ) for the members of the family becomes irrelevant (as was the case for the above choices of the configurations), then monopole scattering looks identical to the scattering of parallel straight strings, and thus the problem simply reduces to the study of string scattering.

B. Skyrmion scattering in 2+1 dimensions

Extension of the above arguments to the case of Skyrmions is then immediate. Since Skyrmions in 2+1 dimensions correspond to nontrivial mapping of S^2 to S^2 , one may try to use the configuration of monopoles of Sec. III A. There is only one subtle point here. A Skyrmion in two space dimensions occurs when fields go to some constant value at the boundary of a closed region. This region then can be considered as the stereographic projection of S^2 , and Skyrmion configuration can be constructed (for more details, see Refs. 21 and 23). Figure 16(a) thus shows a far-separated Skyrmion-anti-Skyrmion pair. These configurations are individually obtained by stereographically projecting the configurations of a monopole [Fig. 14(a)] and of an antimonopole [Fig. 14(b)] onto R^2 . Note the occurrence of region with $\Theta = 0$ in between the Skyrmion-anti-Skyrmion pair. This is one important difference between the case of Skyrmions and the cases of strings and monopoles, where the variation of the Higgs-field phase extends to infinity. Also note that a Skyrmion configuration, contrary to the case of strings and monopoles, does not require that the Higgs field go to zero inside the Skyrmion.

Figure 16(b) shows an intermediate stage of the annihilation [analogous to Fig. 14(c)]. We note that the only

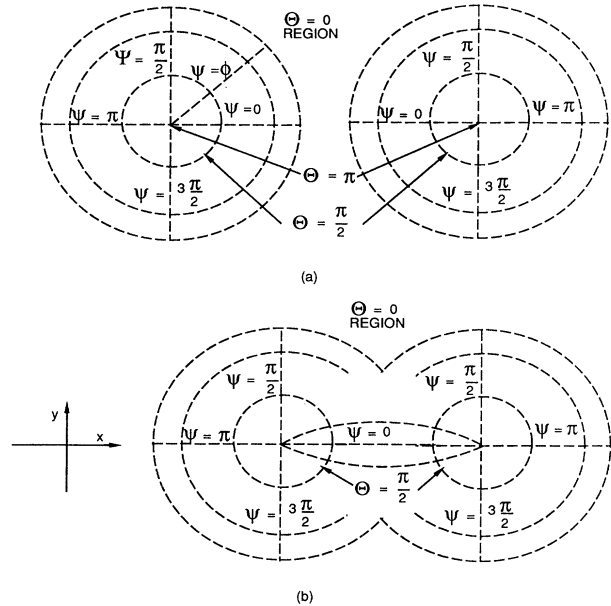


FIG. 16. (a) A far-separated Skyrmion-anti-Skyrmion pair in 2+1 dimensions. (b) An intermediate stage of the annihilation.

difference between the case of string-antistring scattering as shown in Fig. 3(a)–3(c), and this case is the occurrence of another angle Θ which labels different circles around the centers. However we also note that the value of Θ smoothly matches as different circles come into contact. Thus Θ becomes irrelevant (just as Θ became irrelevant for the case of monopoles) reducing this problem to the annihilation of a string-antistring pair. It is easy to see that in the same way the problem of the scattering of a Skyrmion-Skyrmion pair in 2+1 dimensions gets reduced to the case of string-string scattering, and all those results apply to these cases as well.

We, therefore, conclude that a Skyrmion-anti-Skyrmion pair in 2+1 dimensions will bounce back upon annihilation. A Skyrmion-Skyrmion pair will scatter at 90° (a behavior which is very recently observed in certain numerical studies¹³), and the configuration of scattered Skyrmions will be composed of the half-portions of the initial Skyrmions.

C. Skyrmion scattering in 3+1 dimensions

Skyrmions in 3+1 dimensions correspond to a non-trivial mapping of S^3 to S^3 . Following the discussion of Secs. III A and III B, we can construct a Skyrmion by considering the stereographic projection of S^3 . (See Refs. 21 and 23). Figure 17(a) shows a Skyrmion configuration with winding-number one. We see that this is obtained by considering a family of monopole configurations (with unit charge) and labeling each concentric S^2 by a third angle χ between 0 and π . $\chi = \pi$ at the center of the Skyrmion, and χ approaches zero at and beyond the outermost S^2 . Similarly Fig. 17(b) shows an anti-Skyrmion configuration which is obtained from a family of antimonopole configurations. [Again, what we are doing is to start with a winding-number-one (minus one) map of S^2 to S^2 and then extend this map to a winding-number-one (minus one) map of S^3 to S^3 by considering S^3 as a suspension of S^2 .^{21,22,23}

We see that for this choice of Skyrmion configurations, the only difference between the case of monopole-monopole (monopole-antimonopole) scattering and Skyrmion-Skyrmion (Skyrmion-anti-Skyrmion) scattering is the occurrence of another angle χ . However, we also note that the value of χ will smoothly match as different S^2 's come in contact. Thus χ becomes irrelevant (just as Θ became irrelevant for the case of monopoles and for Skyrmions in 2+1 dimensions) reducing the problem to the annihilation of monopole-monopole (monopole-antimonopole) pair.

We, therefore, conclude that a Skyrmion-anti-Skyrmion pair in 3+1 dimensions will bounce back upon annihilation. A Skyrmion-Skyrmion pair will scatter at 90° , and the configuration of scattered Skyrmions will be composed of the half-portions of the initial Skyrmions. What we are finding here is that as far as simple considerations of smooth matching of the Higgs field are concerned, there is virtually no difference between the case of the scattering of strings, monopoles, and Skyrmions. For the choices of the configurations as shown in Figs. 14(a) and 14(b), 16(a), 17(a), and 17(b), we see that

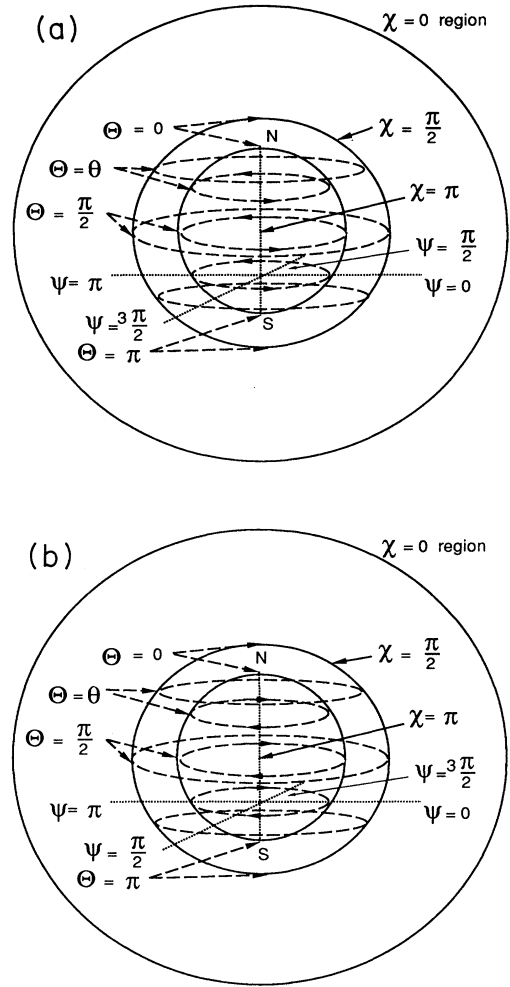


FIG. 17. (a) A Skyrmion and (b) an anti-Skyrmion configuration in 3+1 dimensions.

monopoles as well as Skyrmions in 2+1 dimensions differ from strings due to the existence of another angle Θ , which becomes irrelevant for such scatterings, and Skyrmions in 3+1 dimensions differ from the strings due to two angles Θ and χ , both of which become irrelevant for the above scattering processes. This is the reason why all these objects may be expected to show the same behavior in scattering processes.

IV. CONCLUSIONS

We have considered the scattering of a certain class of global topological defects. These are classified by non-trivial mappings to S^n to S^n with $n = 1, 2$, and 3 , respectively, for strings, monopoles, and Skyrmions in 3+1 dimensions and $n = 1$ and 2 , respectively, for vortices and Skyrmions in 2+1 dimensions. We present *Ansätze* for various stages of the scattering processes, which are motivated by a consideration of the gradient energy. We analyze the configuration at the stage when the two solitons completely overlap, and then by assuming that the consideration of gradient energy determines the dynam-

ics, we draw conclusions about the qualitative aspects of the scattering such as the final direction of scattering. It is clear from our *Ansätze* in various figures that, at the stage of total overlap, the spatial distribution of the magnitude of the Higgs field is roughly symmetric. We expect the magnitude of the Higgs field not to play any important role in determining the direction of scattering and simply concentrate on the spatial variation of the direction of the Higgs field in its vacuum manifold.

We find the surprising result that a string-antistring pair under certain conditions is most likely to scatter back to back. We further argue that a string-string pair will scatter at 90° if the collision is energetic enough so that the string centers overlap at an intermediate stage of the scattering. We find that the scattered string is composed of half-portions of the initial strings. Our *Ansätze* also show why the intercommutivity of strings is expected and how kinks form very naturally at the points where strings intercommuted.

We then show that the scattering processes of monopoles and Skyrmions can be reduced to the scattering of strings under certain conditions. Thus all the qualitative aspects of the scattering of strings automatically apply to the cases of monopole scattering and Skyrmion scattering. This is the most important aspect of our analysis in the sense that even if our arguments for the 90° scattering of strings and back-to-back scattering of a string-antistring pair are not very strong, just by knowing that some of these types of behavior are observed for strings in numerical studies, we can conclude that the same must be true for Skyrmions and monopoles as well. We emphasize here that these results apply to only those scattering processes where Skyrmions (or monopoles) are appropriately oriented.

The 90° scattering of strings and monopoles has been known for some time, and for Skyrmions in $2+1$ dimensions it is observed in very recent numerical simulations. However the back-to-back scattering of these objects is a prediction of our model which has not been observed so far (except in Ref. 6 where a brief mention of such behavior was made for the case of strings). It will be extremely interesting to test these predictions of our analysis in numerical studies by working in an appropriate regime of energy and by working with suitable types of initial configurations. Such a confirmation will be especially important for the case of Skyrmions in $3+1$ dimensions because of possible implications for the nucleon-antinucleon scattering.

Our present analysis is applicable only to global defects as our *Ansätze* are motivated from a consideration of gradient energy. However we know that 90° scattering (as well as intercommutivity of strings) is observed for local strings and monopoles. We thus feel that our approach should be extendible to the case of local strings and

monopoles as well. (Local Skyrmions have zero energy and are of no interest from the point of dynamics.) Another interesting system to study is the scattering of anyons in $2+1$ dimensions. Since anyons in many aspects behave similar to gauged vortices, we expect that same qualitative features may also show up in the scattering of anyons. We are presently working on the investigation of these systems.

As we have discussed, our analysis assumes certain conditions to be valid for the scattering process and hence our predictions are accordingly restricted. For example, for the back-to-back scattering of soliton-antisoliton pairs, we assume that after the initial pair annihilates another pair is recreated. Our qualitative considerations are insufficient to find what sort of initial conditions (for example, the initial energies) are required for this to happen. The situation is somewhat better for 90° scattering of a soliton-soliton pair, where one can say that the initial energies should be large enough that the centers of the solitons completely overlap. However, one has to be careful then whether the dynamics is still dominated by the considerations of gradient energy. In this context we may note that the theoretical investigations of monopole scattering in Refs. 14 and 15 were done for the case of BPS monopoles which do not exert long-range forces on each other. Thus in that case monopoles could overlap even with very small kinetic energies. Similarly the investigation in Refs. 7 and 8 was for the case of critically coupled strings. For the case of the intercommutivity of strings, our considerations (which are based on the gradient energy) will be applicable as long as the relevant kinetic energies are not much larger than the gradient energies.

Our arguments in this paper (for example, for choosing the *Ansätze* for the field configurations) are very intuitive and require stronger justification. However we feel that the strength of our analysis lies in the fact that it provides a common framework for the understanding of many qualitative features of the scattering processes of a large class of topological defects. Some of our results are in complete agreement with the numerical results, and the rest of the results are very clear predictions, the testing of which can provide a clean test of our model.

ACKNOWLEDGMENTS

We would like to thank R. D. Sorkin for useful discussions about the soliton-antisoliton annihilation processes. We also thank A. P. Balachandran and D. Witt for many useful suggestions and comments. The work of C.R. was supported by the DOE under Contract No. DE-FG02-85ER40231. The work of A.M.S. was supported by the Theoretical Physics Institute at the University of Minnesota.

¹N. D. Mermin, *Rev. Mod. Phys.* **51**, 591 (1979).

²For a review, see A. Vilenkin, *Phys. Rep.* **121**, 263 (1985).

³For a review, see A. P. Balachandran, in *High Energy Physics 1985*, Proceedings of the Yale Summer School, New Haven,

Connecticut, 1985, edited by M. J. Bowick and F. Gursev (World Scientific, Singapore, 1986), Vol. 1.

⁴I. Chuang, R. Durrer, N. Turok, and B. Yurke, Princeton University Report No. PUP-TH-1208, 1990 (unpublished).

- ⁵E. P. S. Shellard, Ph.D. thesis, Cambridge University, 1986; Nucl. Phys. **B283**, 624 (1987); other numerical studies of string-antistring interaction include M. W. Hecht and T. A. DeGrand, Phys. Rev. D **42**, 519 (1990).
- ⁶K. J. M. Moriarty, E. Myers, and C. Rebbi, Phys. Lett. B **207**, 411 (1988). There may also be evidence for this back-to-back scattering of high-energy string-antistring pairs in the formation of string loops at high energy; see E. P. S. Shellard, in *Cosmic Strings: The Current Status*, Proceedings of the Yale Workshop, New Haven, Connecticut, 1988, edited by F. S. Accetta and L. M. Krauss (World Scientific, Singapore, 1988); see also R. A. Matzner and J. McCracken, *ibid.*
- ⁷P. J. Ruback, Nucl. Phys. **B296**, 669 (1988).
- ⁸E. P. S. Shellard and P. J. Ruback, Phys. Lett. B **209**, 262 (1988).
- ⁹A. Jackson and A. D. Jackson, Nucl. Phys. **A457**, 687 (1986).
- ¹⁰A. Jackson, A. D. Jackson, and V. Pasquier, Nucl. Phys. **A432**, 567 (1985).
- ¹¹J. J. M. Verbaarschot, T. S. Walhout, J. Wambach, and H. W. Wyld, Nucl. Phys. **A461**, 603 (1987); H. Odawara, O. Morimatsu, and K. Yazaki, Phys. Lett. B **175**, 115 (1986); H. M. Sommermann, H. W. Wyld, and C. J. Pethick, Phys. Rev. Lett. **55**, 476 (1985); M. Karliner and M. P. Mattis, Phys. Rev. D **34**, 1991 (1986); Phys. Rev. Lett. **56**, 428 (1986).
- ¹²U. B. Kaulfuss and Ulf-G. Meissner, Phys. Rev. D **31**, 3024 (1985); A. E. Alder, S. E. Koonin, R. Seki, and H. M. Sommermann, Phys. Rev. Lett. **59**, 2836 (1987).
- ¹³M. Peyrard, B. Piette, and W. J. Zakrzewski, University of Durham Report No. DTP-90/37, 1990 (unpublished).
- ¹⁴N. S. Manton, Phys. Lett. **110B**, 54 (1982); **154B**, 397 (1985).
- ¹⁵M. F. Atiyah and N. J. Hitchin, Phys. Lett. **107A**, 21 (1985).
- ¹⁶J. N. Goldberg, P. S. Jang, S. Y. Park, and K. C. Wali, Phys. Rev. D **18**, 542 (1978); L. O'Raiheartaigh, S. Y. Park, and K. C. Wali, *ibid.* **15**, 1941 (1979).
- ¹⁷M. Temple-Raston, Phys. Lett. B **206**, 503 (1988).
- ¹⁸N. S. Manton, Phys. Lett. B **192**, 177 (1987).
- ¹⁹E. Braaten, Phys. Rev. D **37**, 2026 (1988).
- ²⁰G. J. F. van Heijst and J. B. Flor, Nature **340**, 212 (1989).
- ²¹A. P. Balachandran, A. Daughton, Z. C. Gu, G. Marmo, R. D. Sorkin, and A. M. Srivastava, Syracuse University Report No. SU-4228-433 (unpublished).
- ²²See, for example, D. G. Bourgin, *Modern Algebraic Topology* (MacMillan, New York, 1963).
- ²³A. M. Srivastava, Phys. Rev. D **43**, 1047 (1991).